

Experimental results of helicon sources^{*}

MIAO Ting-Ting(缪婷婷)^{1,2;1)} SHANG Yong(尚勇)^{1,2} LIU Zhan-Wen(刘占稳)¹
 ZHAO Hong-Wei(赵红卫)^{1;2)} SUN Liang-Ting(孙良亭)¹ ZHANG Xue-Zhen(张雪珍)¹
 ZHAO Huan-Yu(赵环昱)¹ WANG Hui(王辉)¹ MA Bao-Hua(马保华)¹ LI Xi-Xia(李锡霞)¹
 ZHU Yu-Hua(朱玉华)¹ FENG Yu-Cheng(冯玉成)¹ LI Jing-Yu(李锦玉)¹

1 (Institute of Modern Physics, Chinese Academy of Sciences, Lanzhou 730000, China)

2 (Graduate University of Chinese Academy of Sciences, Beijing 100049, China)

Abstract Helicon plasma sources are known as efficient generators of uniform and high density plasma. A helicon plasma source was developed for the investigation of plasma stripping and plasma lenses at the Institute of Modern Physics, CAS. In this paper, the characteristics of helicon plasma have been studied by using a Langmuir four-probe and a high plasma density up to $3.9 \times 10^{13}/\text{cm}^3$ has been achieved with the Nagoya type III antenna. In the experiment, several important phenomena were found: (1) for a given magnetic induction intensity, the plasma density became greater with the increase of RF power; (2) helicon mode appeared at RF power between 300 W and 400 W; (3) the plasma density gradually tended to saturation as the RF power increased to the higher power; (4) a higher plasma density can be obtained by a good match between the RF power and the magnetic field distribution. The key issue is how to optimize the matching between the RF power and the magnetic field. Moreover, some tests on the extraction of ion beams were performed, and preliminary results are given. The problems which existed in the helicon ion source will be discussed and the increase in beam density will be expected by extraction system optimum.

Key words helicon sources, plasma density, Langmuir four-probe

PACS 52.25.Jm, 52.50.Qt, 52.55.Jd

1 Introduction

Helicon plasma sources exhibit an excellent capability of producing uniform, high density plasmas up to $10^{13}/\text{cm}^3$, which was first achieved by Boswell in 1968^[1]. Some mechanisms were proposed for coupling the RF power into the plasma in the following years, such as Landau damping suggested by Chen in 1980s^[2] and damping of the evanescent Trivelpiece-Gould (TG) wave on the resonance cone in the 1990s^[3]. Until now, the exact mechanism has not been completely understood^[4], but helicon sources are widely used in various fields such as plasma physics studies, material processing, space propulsion^[5] and accelerator applications in nuclear microprobes and neutron generators, etc^[6]. In this paper, a helicon plasma source was developed for the study of plasma stripping and plasma lenses, and a

helicon ion source was designed for generating intense ion beams. Research groups employing helicon sources have sprung up in Europe, Japan, Korea, and the United States, but they have not been developed in China.

2 Theory of helicon wave

2.1 Dispersion relation

The dispersion relation of the waves which exist in the range $\omega_{ci} \ll \omega_{LH} \ll \omega \ll \omega_{ce} \ll \omega_{pe}$ in the cold plasma can be represented as follows^[7]:

$$\omega = \omega_{ce} \cos \theta \frac{k^2 c^2}{\omega_{pe}^2 + k^2 c^2} \left(1 - i \frac{\nu}{\omega_{ce} \cos \theta} \right), \quad (1)$$

where ω is the angular frequency, ω_{LH} is the lower hybrid frequency, ν is the frequency of electron col-

Received 31 December 2008

^{*} Supported by National Natural Science Funds for Distinguished Young Scholar (10225523)

1) E-mail: miaotingting@impcas.ac.cn

2) E-mail: zhaohw@impcas.ac.cn

©2009 Chinese Physical Society and the Institute of High Energy Physics of the Chinese Academy of Sciences and the Institute of Modern Physics of the Chinese Academy of Sciences and IOP Publishing Ltd

lisions, $\omega_{pe} = (ne^2/\epsilon_0 m)^{1/2}$ is the plasma frequency, $\omega_{ce} = eB/m$ is the electron cyclotron frequency and ω_{ci} is the ion cyclotron frequency, respectively. From Eq. (1), it can be found that the anomalous skin depth, c/ω_{pe} , is the natural boundary of the two different types of wave: helicon and TG waves.

The short wave, $kc \gg \omega_{pe}$, turns out to be strongly damped,

$$\omega = \omega_{ce} \cos \theta - i\nu. \quad (2)$$

These are called TG waves, which are generated in three ways: (1) wave launch by RF current; (2) surface mode conversion; (3) bulk mode conversion.

The long waves, $kc \ll \omega_{pe}$, called helicons, are the right-hand polarized (RHP) waves and propagate in radially confined magnetized plasmas for frequencies $\omega_{ci} \ll \omega \ll \omega_{ce}$,

$$\omega = \omega_{ce} \frac{\cos \theta k^2 c^2}{\omega_{pe}^2} - i\nu \frac{k^2 c^2}{\omega_{pe}^2}. \quad (3)$$

It is clear that the damping of helicons is very weak. When the wave length is of the order of the anomalous skin depth, $kc \approx \omega_{pe}$, the waves of both types merge.

The mode transition from helicons to TG waves may account for efficient ionization, considering the good coupling efficiency with the antenna of the helicon wave and the good electron heating efficiency of the TG wave. Alternatively, the excitation of ion-acoustic parametric turbulence by the primary RF wave in helicon plasmas has been suggested as a possible mechanism for heating electrons and coupling RF power into the plasma^[8].

In a confined plasma, $k^2 = k_{\parallel}^2 + k_{\perp}^2$, $\cos \theta = k_{\parallel}/k$. For a cylinder of radius a aligned with B , the lowest radial mode has k_{\perp} which is approximately equal to p_{11}/a , where $p_{11} = 3.83$ is the first zero root of the Bessel function $J_1(k_{\perp}, r)$. Eq. (3) can then be written as

$$k = \frac{\omega}{k_{\parallel}} \frac{\omega_p^2}{\omega_c c^2} = e\mu_0 v_p \left(\frac{n}{B} \right) \approx \frac{3.83}{a}, \quad (4)$$

$$\frac{B}{n} = 3.12 \times 10^{-3} \cdot E_f^{1/2} \cdot a, \quad (5)$$

$$v_p = \omega/k_{\parallel} = \sqrt{\frac{2eE_f}{m_e}} = f\lambda. \quad (6)$$

where $l_a = \lambda/2$ is the optimum option for the given gas and frequency. From Eqs. (5) and (6), we can obtain the antenna length l_a and discharge tube radius a .

2.2 Antenna coupling

Our studies have been performed with a Nagoya type III antenna designed to excite the $m = +1$ mode

waves^[9] (Fig. 1), where m is the azimuthal mode number. The high efficiency of this antenna can be understood as follows. Consider a time when the current I in Fig. 1 is rising in the direction shown. The rising magnetic field induces a divergence-free electric field E_{em} in the plasma and E_{em} reverses the sign periodically in the z direction. This causes a momentary electron flow which creates a space charge pattern, as indicated by the $+$ and $-$ signs. The space charge, in turn, creates a curl-free electric field E_{es} , shown by the dotted lines, which builds up until the total electric field is parallel to B . Upon reaching the equilibrium, $E_{em} + E_{es}$ is nearly zero in the axial direction. But in the radial direction, E_{em} and E_{es} are in the same direction, the superposition of electric fields forms a transverse electric field. The transverse electric field accelerates the electrons and drives the electron to a high transverse energy.

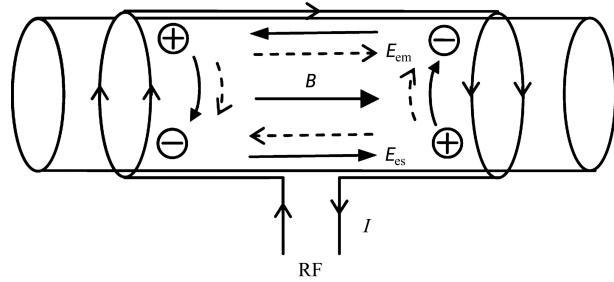


Fig. 1. Coupling theory of Nagoya type III antenna.

According to what is mentioned above, in helicon sources, the multi-mode brings higher RF energy absorption efficiency to the plasma. As a result, the helicon sources have high ionization efficiency, high density plasma and high electron energy.

3 The structures of helicon sources

The helicon plasma source consists of several parts: the discharge chamber, the radio-frequency system, the magnetic system, the plasma diffusion region, the diagnostic system, the vacuum difference system and the pumping system. The experimental setup of the helicon plasma source is shown schematically in Fig. 2.

The helicon ion source (Fig. 3) was constructed on the basis of the helicon plasma source. The diffusion region was substituted by a three electrode beam extraction system^[10]. The dimensions of the extraction system are as follows: the length of plasma electrode is 6 mm and the diameter is 1.5 mm. The ion beam is measured by a Faraday cup.

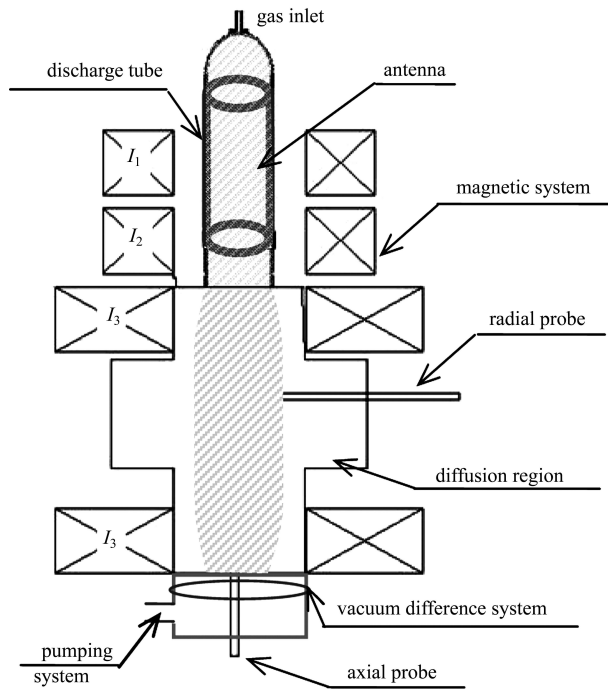


Fig. 2. Helicon plasma source structure.

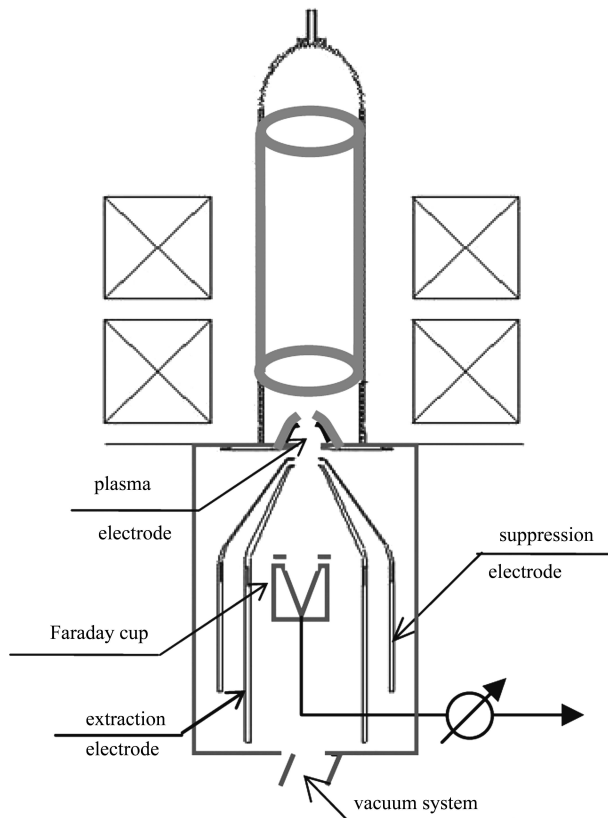


Fig. 3. Helicon ion source structure.

In both of the helicon sources, the discharge chamber is made of a quartz tube with outer diameter of 30 mm and length of 200 mm. Through investigation and preliminary experiments, we found that the uniformly distributed plasma was excited by the helical

antenna and the high density plasma at the center of the chamber was excited by the Nagoya III antenna. Focusing on the high plasma density, the sources were driven by the Nagoya III antenna which generated the right-hand polarized ($m = +1$) azimuthal mode of the helicon wave. The RF power system is composed of a driving generator and a matching box. It can provide a controlled power output of frequency $f_{rf} = 27.12$ MHz in the continuous wave mode. The design of the magnetic system has to meet the following requirements: (1) to generate a magnetic field of strength and distribution resulting in an efficient RF power input into the plasma; (2) to supply a tunable magnetic field; (3) to have a compact structure; (4) to provide optimum beam focusing in the ion source extraction and preliminary acceleration areas. The magnetic field of sources was designed based on calculations with the POISSON-SUPERFISH code. The magnetic coils I_1 and I_2 were designed to supply a magnetic field for uniform longitudinal field or focused field in the extraction region. We can adjust the current of the magnetic coils I_1 and I_2 to obtain a uniform longitudinal magnetic field to generate uniform plasma. We can also optimize the current of coil I_1 to a small value and I_2 to a larger one so as to focus the plasma for beam extraction. The magnetic coil I_3 was designed to supply a uniform longitudinal magnetic field to confine the plasma in the diffusion region. Measurements of the plasma density were performed with a four-Langmuir probe system^[11]. The diameter of the probe is 1 mm and the working portion length is 2 mm. The excellent feature of this probe system is that some parameters such as the electron temperature and plasma density can be obtained directly, without measuring the I - V characteristic curve.

4 Results and discussion

Focusing on achieving high plasma density, a helicon plasma source was designed for the study of plasma stripping and plasma lenses. The plasma density was measured and some characteristics of the plasma were studied.

In the experiment, the argon plasma density from the helicon plasma source was measured by an axial probe at a distance of 3 cm downstream from the end of the antenna. The argon plasma density up to $3.9 \times 10^{13}/\text{cm}^3$ was obtained under the conditions of magnetic intensity 0.02 T, working gas pressure 2.8×10^{-3} Pa and RF power 1200 W. Dependence of the plasma density on the input RF power is shown in Fig. 4.

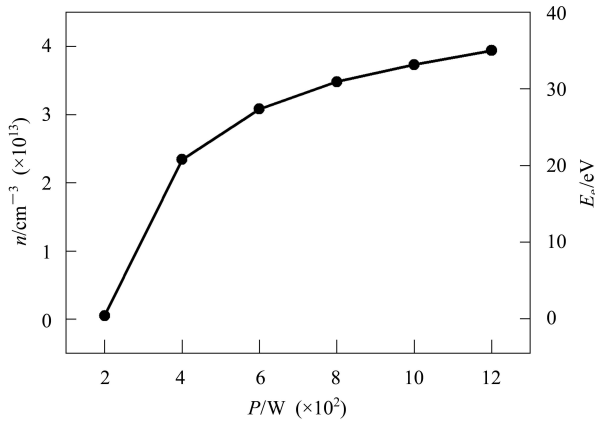


Fig. 4. Density vs. RF power for the Nagoya type III antenna at $B = 0.02$ T, $p = 2.8 \times 10^{-3}$ Pa of argon plasma.

From Fig. 4, some experimental phenomena have been found. (1) For a given magnetic induction intensity, the plasma density becomes greater with the increase of the RF power. The reason is that, under the resonance conditions, the greatest power input is located at the center of the discharge chamber, where more efficient plasma ionization is produced, which results in high plasma density. (2) Jump transition of the plasma density appears at the RF power between 300 W and 400 W, which demonstrates that the helicon mode is produced. (3) The plasma density gradually tends to saturation as the RF power increases, which means that the helicon wave discharge can lead to high ionization efficiency.

Three magnetic coils (I_1 , I_2 and I_3) were added to generate an appropriate axial magnetic field distribution for high plasma density. Fig. 5 shows the plasma density vs. the magnetic induction intensity, which is generated by the magnetic coil I_2 with $I_1 = I_3 = 0$ to produce high plasma density in the extraction region. For a given RF power, the plasma density peak appears at a certain magnetic induction value, and with the different RF power the peaks appear at different magnetic induction. Therefore, we can draw a conclusion that a high plasma density can be obtained by good matching between the RF power and the magnetic induction intensity. The plasma density keeps rising with increasing magnetic induction. This may result from the better plasma radial confinement. In contrast, after the plasma density peak appears, the plasma density decreases as the magnetic induction increases. This could be due to a mirror magnetic field formed at the lower end of the antenna. The ions with high transverse energy are confined and reflected by the mirror magnetic field, and some of the ions flow out of the magnetic mirror escape cone.

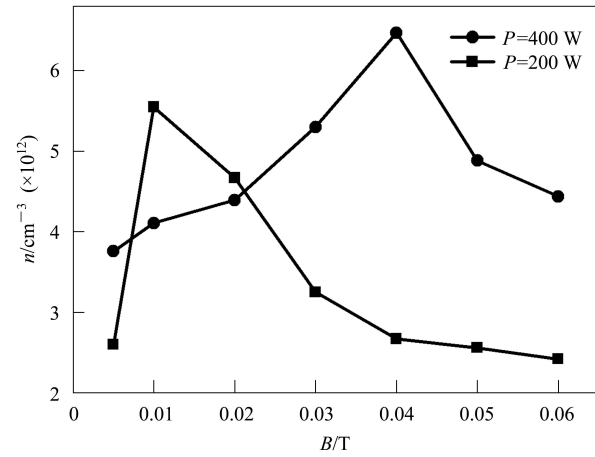


Fig. 5. Plasma density vs. B generated by magnetic coil I_2 with $I_1 = I_3 = 0$ (Fig. 2) at $p = 2.8 \times 10^{-3}$ Pa of argon.

In Fig. 6 the axial and radial plasma density and electron energy profiles are shown respectively. Fig. 6 illustrates that the axial plasma density and the electron energy decline rapidly when the plasmas are ejected out of the emission hole. Besides the electron-ion recombination, this may be because the magnetic field decreases rapidly along the axis, which makes the plasmas diffuse quickly along the radial direction. Measurements of the radial plasma density distribution showed that the radial plasma distributed uniformly in the discharge chamber.

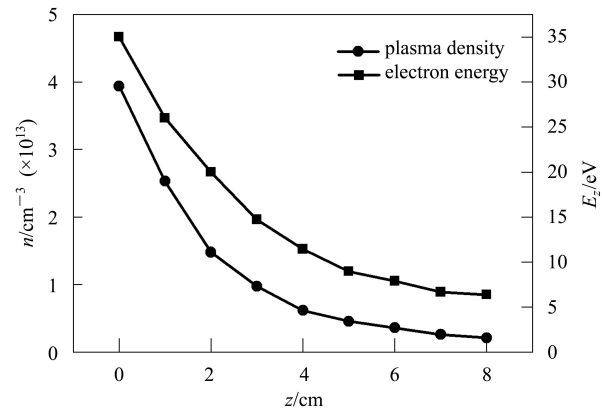


Fig. 6. Axial density and electron energy measured at 3 cm from end of the antenna with $P=1200$ W, $B=0.02$ T, $p=2.8 \times 10^{-3}$ Pa.

Preliminary experiments on the helicon ion source were performed. Some key technical issues have been solved. Firstly, the vacuum seal of the discharge chamber had been solved by shielding the RF field to prevent RF discharge at the vicinity of the “O” ring. Secondly, the extraction electrode was modified to a cone shape, and the plasma electrode was separated from the plasma by a boron nitride disk with a 3 mm hole and 0.5 mm thickness. Therefore,

the power loss and reflection and sputtering problems have been settled.

The extracted argon ion was measured by a Faraday cup. A beam density of 57 mA/cm² for a working gas pressure of 2.1×10^{-4} Pa and on RF power of 400 W was attained. This result is far from what we expected. The reason is that higher transverse electron energy may lead to a larger inherent emittance. On the other hand, the electromagnetic focus system may need to further optimize. In subsequent experiments, a further increase in beam densities would be expected by the ion extraction trajectory simulation and experimental optimum.

5 Conclusion

A helicon plasma source was designed and built successfully. A plasma density up to 3.9×10^{13} /cm³ has been measured by an axial Langmuir four-probe under the conditions of a magnetic intensity of 0.02 T, a working gas pressure of 2.8×10^{-3} Pa and an RF power of 1200 W. The characteristics of the

helicon plasma were studied and some experimental phenomena found. (1) For a given magnetic induction intensity, the plasma density became greater with the increase of RF power. (2) The helicon mode appeared at the RF power between 300 W and 400 W. (3) The plasma density gradually tended to saturation as the RF power increased to a higher power. (4) A higher plasma density could be obtained by good matching between the RF power and the magnetic field distribution. The key issue is how to optimize the matching between the RF power and the magnetic field. An argon beam density of 57 mA/cm² for a working gas pressure of 2.1×10^{-4} Pa and an RF power of 400 W was obtained. To achieve higher plasma density and more intense ion beams, further improvements and systematic experiments will have to be conducted in the future.

The authors are grateful to Wan Baonian at the Institute of Plasma Physics for plasma diagnosis and Shi Aimin at the Institute of Modern Physics for impedance matching.

References

- 1 CHEN F F, Boswell R W. IEEE Transactions on Plasma Science, 1997, **25**(6): 1245
- 2 CHEN F F. Plasma Physics and Controlled Fusion, 1991, **33**(4): 339
- 3 Arnush D, CHEN F F. Physics of Plasmas, 1998, **5**(5): 1239
- 4 Scime E E, Keesee A M, Boswell R W. Physics of Plasmas, 2008, **15**(5): 058301
- 5 Squirea J P, Chang-Díaza F R, Glover T W et al. Thin Solid Films, 2006, **506-507**: 579
- 6 Mordyk S, Miroshnichenko V, Shulha D. Rev. Sci. Instrum., 2008, **79**(2): 02B707
- 7 Shamrai P Konstantin, Taranov B Vladimir. Plasma Sources Sci. Technol., 1996, **5**: 474
- 8 Lorenz B, Krämer M, Selenin V L et al. Plasma Sources Sci. Technol., 2005, **14**(3): 623
- 9 Miljak David G, CHEN F F. Plasma Sources Sci. Technol., 1998, **7**: 61
- 10 Alton G D, Bilheux H. HEP & NP, 2007, **31**(Supp.1): 201 (in Chinese)
- 11 XU G S, WAN B N. Plasma Science & Technology, 2006, **8**(1): 10